Temperature and fuel availability control fire size/severity in the boreal forest of central Northwest Territories, Canada

Dorian M. Gaboriau, Cécile C. Remy, Martin P. Girardin, Hugo Asselin, Christelle Hély, Yves Bergeron, Adam A. Ali

Temperature and fuel availability control fire size/severity in the boreal forest of central Northwest Territories, Canada

Dorian M. Gaboriau[1,2], Cécile C. Remy[3], Martin P. Girardin[4,5], Hugo Asselin[1,4], Christelle Hély[2,6,7], Yves Bergeron[4,7], Adam A. Ali[2,7]

[1]School of Indigenous Studies, Université du Québec en Abitibi-Témiscamingue, 445 Boulevard de l'Université, Rouyn-Noranda, QC, J9X 5E4, Canada

[2]Institut des Sciences de l'Evolution, UMR 5554 CNRS-IRD-Université Montpellier-EPHE, 2 place Eugène Bataillon, 34095 Montpellier, France

[3]Department of Biology, University of New Mexico, Albuquerque, United States

[4]Centre for Forest Research, Université du Québec à Montréal, P.O. Box 8888, Stn. Centre-ville, Montréal, QC, H3C 3P8, Canada

[5]Natural Resources Canada, Canadian Forest Service, Laurentian Forestry Centre, 1055 rue du PEPS, P.O. Box 10380, Stn. Sainte-Foy, Québec, QC, G1V 4C7, Canada

[6]École Pratique des Hautes Études, PSL University, Paris, France

[7]Forest Research Institute, Université du Québec en Abitibi-Témiscamingue, 445 Boulevard de l'Université, Rouyn-Noranda, QC, J9X 5E4, Canada

Corresponding author

dorian.gaboriau@uqat.ca

Abstract

The north-central Canadian boreal forest experienced increased occurrence of large and severe wildfires caused by unusually warm temperatures and drought events during the last decade. It is, however, difficult to assess the exceptional nature of this recent wildfire activity, as few long-term records are available in the area. We analyzed macroscopic sedimentary charcoal from four lakes and pollen grains from one of those lakes to reconstruct long-term fire regimes and vegetation histories in the boreal forest of central Northwest Territories. We used regional estimates of past temperature and hydrological changes to identify the climatic drivers of fire activity over the past 10,000 years. Fires were larger and more severe during warm periods (before *ca.* 5,000 cal. yrs. BP and during the last 500 years) and when the forest landscape was characterized by high fuel abundance, especially fire-prone spruce. In contrast, colder conditions combined with landscape opening (i.e., lower fuel abundance) during the Neoglacial (after *ca.* 5,000 cal. yrs. BP) were related with a decline in fire size and severity. Fire size and severity increased during the last five centuries, but remained within the Holocene range of variability. According to climatic projections, fire size and severity will likely continue to increase in central Northwest Territories in response to warmer conditions, but precipitation variability, combined with increased abundance of deciduous species or opening of the landscape, could limit fire risk in the future.

Keywords

large wildfires; charcoal; pollen; fire size; lake sediments; vegetation dynamics; climate change; Holocene

1. Introduction

The global climate is experiencing rapid warming conducive to increased occurrence of extreme weather events like heatwaves and droughts (IPCC, 2014; Mann et al., 2017). Such conditions may increase the occurrence of exceptionally large and severe wildfires due to the strong positive correlation between temperature and area burned (Abatzoglou and Kolden, 2013; Ali et al., 2012; Duffy et al., 2005; Gaboriau et al., under review; Kasischke and Turetsky, 2006; Turco et al., 2017). Particularly high temperatures and recurrent droughts during the last decade have led to severe wildfire seasons in forest ecosystems worldwide, for example in Australia (Boer et al., 2020; Nolan et al., 2020), Sweden (SFOR, 2018), Chile (De la Barrera et al., 2018), Greece and the USA (Smith et al., 2019), as well as in the Northwest Territories (NWT) in Canada where about 3.4 million ha burned during the summer of 2014 (Kochtubajda et al., 2019; NTENR, 2015).

Large wildfires in the NWT mainly occur from June to September. Lightning-induced fires are predominant and fire frequency and area burned are among the highest in the North American boreal forest (Erni et al., 2020; Veraverbeke et al., 2017). However, the 2014 wildfire season was exceptional in comparison with observations of the last decade (3.4 million ha burned in 2014, compared to a mean of 622 thousand hectares burned annually from 2009 to 2019; Gaboriau et al., under review). More than 380 fires were observed, some of which having burned more than 150,000 hectares. Moreover, firefighting costs reached more than CAD 56 million during this exceptional year, compared to an annual mean of CAD 7.5 million in the previous 20 years (NTENR, 2015).

Few remnant trees are left behind in areas burned during large and severe wildfires (Erni et al., 2017; Stephens et al., 2014). Recolonization is dominated by fast-growing pioneer deciduous tree species whose seeds disperse over long distances (Chapin et al., 2010; Walker et al., 2018). Large wildfires also reduce access to ecosystem services (Adams, 2013), cause health issues in human

67 populations (Dodd et al., 2018), and decrease the capacity of Indigenous people to maintain traditional
68 activities on the land (Berkes and Davidson-Hunt, 2006).

69 Since the 1950s, mean annual temperature increased by over 1.5°C in Canada, leading to an
70 earlier onset of snowmelt across much of the boreal forest (Zhang et al., 2011). According to climate
71 projections, temperature will continue to rise in the next decades, particularly in the north-central
72 Canadian boreal forest (Price et al., 2013; Wang et al., 2014). Summer and fall precipitation are
73 projected to increase in the boreal forest of Canada and annual precipitation could increase up to 20% by
74 2100. However, these conditions will not necessarily lead to increased soil and vegetation moisture, as
75 projected warmer temperatures will lead to increased evapotranspiration (IPCC, 2014; Meehl et al.,
76 2007). Hence, the drying effect of higher temperatures in the future will not necessarily be compensated
77 by increased precipitation. Boreal forest landscapes will consequently be altered by a longer growing
78 season (Jain et al., 2018), increased fire activity (Flannigan et al., 2013; Hassol, 2005; Wang et al., 2017;
79 Wotton et al., 2017), higher proportion of deciduous tree species and more open forest canopies than
80 currently (Baltzer et al., submitted; Boulanger et al., 2017; Chaste et al., 2019; Mekonnen et al., 2019).
81 However, the robustness of the predictions of climate change impacts on wildfire regimes, particularly
82 large wildfires, is limited by our lack of knowledge of the long-term interactions between climate,
83 vegetation and fire (Ali et al., 2012; Conedera et al., 2009; Coogan et al., 2019). While the main drivers
84 of fire activity have been documented in the NWT for the recent past (1965-2016; Gaboriau et al.,
85 submitted), few palaeoecological data are available at multi-millennial timescales.

86 To get insights into the long-term relationships between climate, vegetation and fire, we used
87 high-resolution sedimentary proxies (pollen grains and charcoal particles) to reconstruct vegetation and
88 fire histories for the past 10,000 years in the boreal forest of central NWT. We compared the
89 reconstructed vegetation and fire histories with previous studies based on regional climatic

reconstructions. Our objectives were (1) to determine whether the recent wildfire regime (last 500 years) is within or outside the Holocene range of variability and (2) to decipher the respective roles of climate and vegetation controls on past fire activity. We expected that the recent fire regime would be characterized by larger and/or more severe wildfires compared to the past 10,000 years in response to ongoing climate warming and recurrent development of severe drought episodes.

2. Material and methods

2.1. Study area and present-day vegetation

We sampled sediments from lakes *Emile*, *Izaac*, *Paradis* and *Saxon* (unofficial names) located north of Yellowknife, in central NWT, and 5-100 km distant from each other (Fig. 1). The sampled lakes have a mean elevation of 382 m (Table 1). According to the Canadian National Fire Database (CNFDB, http://cwfis.cfs.nrcan.gc.ca/ha/nfdb), time since the last fire varied between 4 and 39 years in the watersheds of the studied lakes (Table 1). The regional climate is dry continental, with long cold winters and short warm summers (Environnement Canada, 2017). The study area is located close to the treeline (Timoney et al., 2019) and is part of the Taiga Boreal Shield West ecoregion, characterized by rock outcrops and discontinuous permafrost (Olson et al., 2001). Vegetation is currently dominated by conifer tree species, mostly black spruce (*Picea mariana* (Mill.) B.S.P.). White spruce (*Picea glauca* (Moench) Voss.) is mainly found in the southwestern part of the study area, and jack pine (*Pinus banksiana* Lamb.) mostly occupies the southern part of the NWT, *i.e.* in the Taiga Plains. Broadleaf tree species are also present in younger stands having regenerated after fire, mostly paper birch (*Betula papyrifera* Marsh) and trembling aspen (*Populus tremuloides* Michx.), such as observed at lake *Emile* (Appendix S1A). The shrub layer is mainly composed of *Betula glandulosa* Michx., *Alnus alnobetula* (Ehrh.) K. Köch, *Andromeda polifolia* L., *Ledum palustre* L., and *Chamaedaphne calyculata* (L.) Moench. The ground layer is mostly composed of *Vaccinium vitis-idaea* L., *Rubus chamaemorus* L., *Kalmia*

angustifolia L. and *Lycopodium annotinum* L., with abundant mosses (mostly *Sphagnum* spp.), while *Cladonia* lichens are found on xeric rock outcrops.

2.2. Past regional climate and vegetation

Previous studies have documented long-term regional climatic and vegetation changes in the northwestern and north-central Canadian boreal forest, which in turn had impacts on wildfire regimes. Before *ca.* 11,000 cal. yrs. BP (calibrated years before present), high solar radiation and summer insolation increased temperatures in the northwestern Canada (Viau et al., 2006), reduced snow cover, and led to the retreat of the Laurentide ice sheet (Dyke, 2005). Deglaciation occurred between *ca.* 10,000 – 9,000 cal. yrs. BP in the study area (Dalton et al., 2020) and left behind numerous lakes and swamps scattered across the landscape (Latifovic et al., 2017; MacDonald, 1995). Following ice retreat, the land was quickly colonized by tundra vegetation soon followed by trees once temperatures warmed during the early Holocene (Dyke, 2005). The Holocene Thermal Maximum (HTM) occurred in northern continental Canada during the mid-Holocene (between 7,300 and 4,300 cal. yrs. BP; Kaufman et al., 2004). During this period, major vegetation reorganization occurred in response to warmer temperature, such as treeline migration to the north and increased abundance of fire-adapted species (i.e. jack pine and black spruce), as observed in the NWT and southwestern Yukon (Gajewski et al., 2014; Pienitz et al., 1999; Sulphur et al., 2016). The decrease in temperature after 4,300 cal. yrs. BP, characterizing the Neoglacial period, favored coniferous species such as spruce as well as deciduous shade-tolerant tree species such as paper birch in permafrost-free areas (Moser and MacDonald, 1990; Sulphur et al., 2016). However, interactions between climate, vegetation and fire depend on regional atmospheric and oceanic oscillations, as observed in the eastern Canadian boreal forest where conifer species also increased in density after 3,500 cal. yrs. BP (Fréchette et al., 2018; Remy et al., 2017).

135 *2.3. Sampling*

136 We sampled lake sediments in June 2018 from the deepest point in each of the four lakes. The
137 vegetation of the watersheds was mainly composed of recently burned conifer tree species and/or shrub
138 birch having grown after the last fire (Appendix S1). The four lakes were small, deep, circular, and
139 characterized by the absence of connections to surrounding watercourses (Table 1). We used a Kajak-
140 Brinkhurst (KB) gravity corer to collect the most recently deposited material at the water-sediment
141 interface (Glew 1991). We subsampled surface sediments on site in 0.5-cm thick sections stocked in
142 plastic bags. We collected deeper sediments in 1-m cores using a 5-cm diameter Russian corer; we
143 wrapped these cores in aluminum foil and placed them in hemicylindrical tubes for protection. We sliced
144 the sediment cores in the laboratory into continuous 1-cm thick subsamples that we stocked in plastic
145 bags and kept refrigerated at 4°C until analysis. Surface sediments were sampled at a shorter interval
146 (0.5cm) than deeper sediments (1 cm) to ease comparison with recent (last 500 years) reconstructions of
147 vegetation and fire history.

148 *2.4. Radiocarbon dating and age-depth models*

149 The basal 10 cm of the deepest sediment cores were mostly clay, corresponding to the beginning
150 of lake sedimentation following deglaciation in the four sites, whereas the upper sediment was
151 composed of a gyttja richer in organic matter. We constructed core chronologies based on radiocarbon
152 dating of bulk gyttja samples by ^{14}C accelerator mass spectrometry (AMS). We used the '*WinBacon*'
153 v.2.3.7 R package (Blaauw and Christen, 2011) to reconstruct Bayesian sediment accumulation histories
154 and calibrate age-depth models constructed from seven dates for lakes *Emile*, *Paradis* and *Saxon* and
155 nine dates for lake *Izaac* (Table S1). We used the IntCal13.14C calibration curve for terrestrial northern
156 hemisphere material (Reimer et al., 2013). We interpolated ages at contiguous 0.5-cm depth intervals
157 and all dates were expressed in calibrated years before present (cal. yrs. BP). We used linear

158 interpolation between ^{14}C ages rather than best-fit curves, assuming that both methods yield equivalent
159 chronologies (Blaauw, 2010; Trachsel and Telford, 2017).

160 *2.5. Subsample chemical preparation and charcoal analysis*

161 To distinguish charcoal from other biological material, we applied a common charcoal extraction
162 protocol to each subsample using the 'chemical digestion' method (Winkler, 1985), based on charcoal
163 resistance to chemicals (Mooney and Tinner, 2011). We removed a 1.4-cm^3 subsample from each liquid
164 subsample of surface sediment (KB) and 1-cm^3 for the rest of the core (solid part), following Mustaphi
165 et al. (2015). We took sediments in the central part of each core slice to limit the risk of contamination
166 with modern material. We deflocculated and bleached the subsamples by placing them in a potassium
167 hydroxide (KOH) solution combined with bleach and sodium hexametaphosphate – $(NaPO_3)_6$ – on a
168 stirring table for 24 hours at room temperature; which later allowed us to differentiate black charcoal
169 from bleached organic matter (Braadbaart and Poole, 2008; Swain, 1973). We wet-sieved the solution
170 through a 160 µm mesh to collect larger charcoal particles produced by fire events having mostly
171 occurred 0-3 km from the lakeshore (Oris et al., 2014). We sorted charcoal particles in a Petri dish, and
172 measured their area using a camera (D-Moticam 1080, Motic Images, 2018) mounted on a binocular
173 microscope and connected to an image-analysis software (MOTICAM IMAGE Plus 3.0).

174 *2.6. Fire history reconstruction*

175 We reconstructed burned biomass (hereafter *BB*; unitless) at each study site by measuring the
176 cumulative area of charcoal particles per cm^3 for each subsample. Based on numerical age-depth
177 models, we transformed this measure into charcoal accumulation rate (hereafter CHAR, i.e. $mm^2\ cm^{-2}$
178 yr^{-1}), using the R package '*paleofire'* v.1.2.3 (Blarquez et al., 2014). We pooled and smoothed these
179 series (using a 500-year window) by (1) rescaling initial CHAR values using min-max transformation,
180 (2) homogenizing the variance using Box-Cox transformation, and (3) rescaling the values to Z-scores

(Power et al., 2008). The resulting values (cumulative charcoal area) are interpreted as representing the regional signature of fires having occurred in the watersheds of the studied lakes, and thus the regional burned biomass (hereafter *RegBB*; unitless).

We detected past fire events (Appendix S2) within each individual CHAR series using the CharAnalysis v.1.1 software (Higuera, 2009; available at https://github.com/phiguera/CharAnalysis). Following Brossier et al. (2014), we used the narrowest time window allowing us to obtain a median Signal-to-Noise Index greater than 3.0 (Table 1). We obtained the past regional fire frequency (hereafter *RegFF*; fire.year^{-1}) by combining the smoothed series using the R package '*paleofire'* v.1.2.3 (Blarquez et al., 2014). We assessed the significance of changes in *RegFF* and *RegBB* by using a bootstrap procedure with 999 iterations (BCI; 90%).

Following Ali et al. (2012), we added a constant equal to 1 to *RegBB* and *RegFF* and we computed the ratio (*FS* index), which we interpreted as indicating fire size and/or severity. The *FS* index corresponds to mean burned biomass per fire calculated for 500-year intervals, and thus, reflects fire size. Considering that large fires in boreal North America are known to cause high vegetation mortality, the *FS* index could also represent fire severity (Ali et al., 2012; Cansler and McKenzie, 2014; Hély et al., 2020; Hennebelle et al., 2020; Kelly et al., 2013). We assumed that high *FS* index values corresponded to periods when the study area experienced larger and more severe wildfires. Following Power et al. (2008), we used a reference period, here corresponding to 500-0 cal. yrs. BP (by convention, 0 cal. yr. BP corresponding to AD 1950), to calculate *RegBB*, *RegFF* and *FS* index anomalies.

2.7. Vegetation history reconstruction

We reconstructed the Holocene vegetation history using palynological analysis of subsamples of bulk sediment (1 cm^3) taken at regular 4 cm intervals along the core of lake *Emile*. We counted and determined pollen and spores in sediment subsamples using standard techniques described by Faegri and

204 Iversen, (1989). We counted a minimum of 300 pollen grains of terrestrial taxa for each subsample
205 (Djamali and Cilleros, 2020), under a microscope with a × 200 or × 400 magnification factor. We
206 identified pollen grains based on the Pollen Atlas of Arctic and Boreal Canada (Williams, 2006) and
207 pollen keys from (Vincent, 1973) and Richard (1970). We identified tree pollen to the genus level. We
208 also identified the green algae *Pediastrum* and spores of aquatic plants. We added exotic marker pollen
209 (*Eucalyptus*) to each subsample to estimate pollen concentration (grains cm^3) and pollen accumulation
210 rate (*n* grains cm^{-2} yr^{-1}) for taxa with an average percentage greater than 0.1% (Appendix S3), using the
211 R package 'rioja' (Juggins, 2017). We measured the total pollen accumulation rate (PAR), based on all
212 terrestrial taxa with percentages greater than 0.1%.

213 *2.8. Temperature and drought*

214 We used quantitative temperature reconstructions from four different proxies (described in Appendix
215 S4) and originating from northwestern and north-central Canada (Lecavalier et al., 2017; Porter et al.,
216 2019; Upiter et al., 2014; Viau et al., 2006). The reconstructions included (i) mean air temperature in
217 July from 6,000 cal. yrs. BP to present estimated from chironomid assemblages sampled in lake
218 sediments of the central Northwest Territories (Upiter et al., 2014), (ii) mean summer temperature
219 anomalies relative to the 1961-1990 period in central Yukon, from 10,000 cal. yrs. BP to present,
220 estimated using precipitation isotopes in syngenetic permafrost (Porter et al., 2019), (iii) mean Arctic
221 summer air temperature anomalies relative to the preindustrial period reconstructed from ice melt in the
222 Agassiz ice cap (Ellesmere Island, Northwest Territories) (Lecavalier et al., 2017), and (iv) mean July
223 temperature estimated from pollen records for the past 10,000 years across northwestern North America
224 (Viau et al., 2006). We assumed that these reconstructions captured temperature fluctuations during the
225 summer months, i.e. the period of warm and dry weather conducive to wildfire activity in the boreal
226 forest. For each reconstruction, we interpolated and standardized values for each year between 10,000

227 cal. yrs. BP and present, converting the data in anomalies relative to the mean for the entire period. We
228 then averaged the four reconstructions. Then, we assessed the significance of temporal changes in
229 temperature by bootstrapping the pooled means 999 times (BCI; 90%). We present temperature
230 anomalies relative to the reference period 500-0 cal. yrs. BP.

231 To quantify the relationships among the fire, vegetation and temperature time series reconstructed at
232 different temporal resolutions, and to avoid interpolation when time series were not sampled at identical
233 points, we measured the Pearson correlation coefficient with 95% confidence interval between the
234 automatically binned undetrended time series following Mudelsee (2013) and using the R package
235 'BINCOR' (Polanco-Martinez et al., 2019).

236 We used three indicators of hydrological variability to define Holocene dryness periods assumed to
237 correspond to low vegetation productivity (inferred from pollen and plant macrofossil assemblages) and
238 low lake water levels (inferred from diatoms) (Lauriol et al., 2009; Pienitz et al., 1999; Viau and
239 Gajewski, 2009). We compared these records providing independent evidence of dryness periods with
240 our fire reconstructions to detect possible temporal overlap of specific fire regimes and dryness periods.

241 **3. Results**

242 *3.1. Age-depth models*

243 Core length varied from 359 cm at lake *Izaac* to 456 cm at lake *Emile* (Table S1). According to the
244 Bayesian age-depth models, basal sediments were dated between *ca.* 10,000 cal. yrs. BP at lake *Saxon*
245 and *ca.* 9,530 cal. yrs. BP at lake *Izaac* (Fig. 2). We used 9,530 cal. yrs. BP as the earliest date for
246 wildfire regime reconstructions, as it was included in all four reconstructions. The four age-depth
247 models had similar sedimentation rates, varying between 0.036 cm and 0.049 cm $year^{-1}$ (Table 1),
248 similar to the results a previous study of other boreal lakes in the NWT (Crann et al., 2015).

3.2. Regional fire history

The regional fire activity remained fairly constant throughout the Holocene with approximately 5 fires per millennium (+2 anomaly; Fig. 3A). Mean *RegFF* very slightly increased from *ca.* 9,500 cal. yrs. BP to *ca.* 500 cal. yrs. BP, before decreasing during the reference period (500-0 cal. BP). *RegBB* steadily increased starting from *ca.* 9,500 cal. yrs. BP, peaked between *ca.* 7,000-5,000 cal. yrs. BP, before gradually decreasing to present values, the lowest of the entire series (Fig. 3B). Higher *FS* index values were recorded before 4,000 cal. yrs. BP (Fig. 3C), and, although to a lesser extent, during the reference period (500-0 cal. yrs. BP).

3.3. Vegetation history

We identified a total of 41 pollen taxa in the whole sequence extracted at lake *Emile*, covering the period from *ca.* 9,700 cal. yrs. BP to present. Eighteen taxa had a mean pollen percentage > 0.1% over the entire study period (Appendix S3). The PAR diagram is dominated by few tree and shrub taxa throughout the sequence (*Picea*, *Betula, Pinus* and *Alnus*; Fig. 4). *Artemisia*, Cyperaceae, Ericaceae, Poaceae, *Juniperus*, *Larix* and *Salix* were also present, but in low numbers.

PAR was low from *ca.* 9,700 to 7,800 cal. yrs. BP, concomitant with a stable and relatively low sedimentation rate (Fig. 4). Most trees and shrubs were relatively low, except *Populus, Myrica* and *Lycopodium*, which recorded their highest values at that time. A marked increase of *Picea* (likely black spruce, MacDonald et al., 1993) occurred *ca.* 7,800 cal. yrs. BP, along with a simultaneous expansion of *Alnus alnobetula* subsp. *crispa*. At the same time, the lake recorded a major decrease in *Populus*, *Myrica* and *Lycopodium*. PAR increased markedly, while the sedimentation rate remained stable. PAR, *Picea* and *Alnus alnobetula* subsp. *crispa* remained high until *ca.* 6,000 cal. yrs. BP, before decreasing, concomitant with an increase of the sedimentation rate ca. 5,700 cal. yrs. BP. *Pinus* (likely jack pine; Sulphur et al., 2016), *Betula* and *Alnus incana* subsp. *rugosa* increased somewhat later, while the

sedimentation rate remained high. After *ca.* 4,000 cal. yrs. BP, the sedimentation rate decreased and remained stable for the last two millennia of the record, while *Pinus* remained relatively high, especially after *ca.* 2,500 cal. yrs. BP. A short-duration PAR peak occurred between *ca.* 3,000 and 2,200 cal. yrs. BP, although the sedimentation rate remained stable. *Pediastrum* and *Nuphar* increased simultaneously *ca.* 2,200 cal. yrs. BP. During the last two millennia, *Picea*, *Pinus*, *Betula* and *Alnus* sp. decreased, while Ericaceae and Cyperaceae remained stable or even slightly increased, such as for *Juniperus*. The sedimentation rate decreased after 500 cal. yrs. BP, following a slight increase between *ca.* 1,500 and 500 cal. yrs. BP.

3.4. Temperature and drought

We identified three main climatic periods over the Holocene, based on pooled summer temperature reconstructions (Fig. 5). Larger confidence intervals reveal more uncertainty in temperature estimations from 10,000 to 6,500 cal. yrs. BP, corresponding to the early Holocene period. Overall, maximum temperature values were recorded between *ca*. 6,500 and 4,500 cal. yrs. BP, before decreasing until *ca.* 1,500 cal. yrs. BP, and increasing again drastically during the last few centuries. According to inferred hydrological conditions (Fig. 6; Lauriol et al., 2009; Pienitz et al., 1999; Viau and Gajewski, 2009), the period between *ca.* 7,000-3,000 cal. yrs. BP was characterized by wetter conditions in central NWT and northern Yukon, compared to the rest of the study period. A major change in diatom-inferred dissolved organic carbon at *ca.* 5,800 cal. yrs. BP suggests a warm and humid interval during the mid-Holocene (Fig. 6a; Pienitz et al., 1999), resulting in high lake productivity (Fig. 6c; Lauriol et al., 2009). Conversely, high annual precipitation were recorded before *ca.* 7,500 cal. yrs. BP and around *ca.* 1,000 cal. yrs. BP (Fig. 6b; Viau and Gajewski, 2009).

293 *3.5. Relationships between fire, temperature and vegetation*

294 Warm periods (*ca*. 10,000 to 5,000 cal. yrs. BP and last 500 years) coincided with low *RegFF*, high
295 *FS* index, and relatively high *RegBB* (Table 2). Higher temperatures corresponded with higher *Populus*,
296 *Myrica* and *Lycopodium* abundance. A cooler period (*ca*. 5,000 to 500 cal. yrs. BP) was characterized by
297 a low *FS* index and a landscape richer in *Pinus*, *Larix*, *Juniperus*, Poaceae, *Pediastrum* and *Nuphar*
298 (Table 2). PAR, interpreted as fuel availability, coincided with high *RegFF* and high *RegBB*, especially
299 for *Picea*, *Betula* and *Alnus alnobetula* subsp. *crispa* (Table 2).

300 **4. Discussion**

301 Our fire history reconstructions based on macroscopic sedimentary charcoal provide evidence that
302 fire size and/or severity were higher during warmer periods (i.e. before *ca.* 5,000 cal. yrs. BP and during
303 the last 500 years) than during the Neoglacial (after *ca.* 5,000 cal. yrs. BP). During the Holocene, the
304 *RegBB* metric was positively correlated with the *FS* index because *RegFF* was relatively constant from
305 the early to the late Holocene.

306 *4.1. Fire, climate and vegetation interactions*

307 *Early Holocene (10,000-6,500 cal. yrs. BP)*

308 The spatial variability of the climate data used in air temperature reconstructions shown by the large
309 confidence interval around summer temperature during the early Holocene (i.e. before 6,500 cal. yrs.
310 BP; Figure 5) is due to differences in time of deglaciation across northern Canada (Dyke, 2005;
311 Kaufman et al., 2004). Summers were warmer in far northern NWT and in central Yukon (Lecavalier et
312 al., 2017; Porter et al., 2019) but cooler in northwestern Canada (Viau et al., 2006), probably due to a
313 later time of deglaciation. Conditions were also dry at this time in north-central Canada but not in
314 northwestern Canada (i.e. Mackenzie region; Fig. 6), confirming the presence of the Laurentide ice sheet
315 in the study area during the early Holocene. PAR indicates that the first stage of vegetation colonization

316 following ice retreat was characterized by an open woodland, as observed in previous studies for the
317 same period and in the same area (Conedera et al., 2009; Macumber et al., 2011; Sulphur et al., 2016).
318 The landscape was dominated by pioneer taxa such as *Populus* and *Betula* (likely dwarf birch, Andrews
319 et al., 1980). The relatively high percentages of *Picea* spp. (~ 40-50 %) was likely due to long-distance
320 transport of pollen by wind, from populations located to the southwest of the study area (Campbell et al.,
321 1999). Low tree abundance before 8,000 cal. yrs. BP can be explained by the time required for
322 northward migration following deglaciation (Gajewski et al., 1993; Moser and MacDonald, 1990;
323 Ritchie, 1985). Dry conditions also could have limited tree cover. During the early Holocene, deciduous
324 shrubs, less inflammable than conifer trees, and low fuel abundance likely limited fire ignition and
325 spread, but might have promoted large and/or severe fires in shrub areas during dry years.

326 *Mid-Holocene (6,500-5,000 cal. yrs. BP)*

327 Warmer and wetter climate during the mid-Holocene in northern continental Canada (Kaufman et al.,
328 2004; Porter et al., 2019; Ritchie et al., 1983) favored tree growth, leading to gradual densification of the
329 vegetation cover as suggested by the increase in PAR values despite a relatively stable sedimentation
330 rate. This result is in line with previous reconstructions in southwestern Yukon (Cwynar and Spear,
331 1995; Gajewski et al., 2014), Alaska (Tinner et al., 2006) and Northwest Territories (Sulphur et al.,
332 2016). Warm temperature and wet conditions of the mid-Holocene especially favored dense conifer
333 forests (*Picea* and *Pinus spp.*), causing fuel accumulation conducive to large and severe fires, as
334 previously observed in Alaska (Hoecker et al., 2020). During this period, wet conditions limited the
335 increase in fire frequency (*RegFF*), which remained stable, while biomass burning (*RegBB*) was higher.
336 Because the period was wet, it suggests that these non-frequent large wildfires occurred during episodic
337 drought that dried the fuel and favored fire spread. High fire activity during the mid-Holocene promoted

fire-prone coniferous species (*Picea* and *Pinus*) and pioneer trees and shrubs (*Betula* and *Alnus*), as previously observed in the study area (Parisien et al., 2020).

Neoglacial (5,000-1,000 cal. yrs. BP)

The Neoglacial was characterized by a gradual decrease in temperature, reaching an all-time low *ca.* 1,500 cal. yrs. BP. Cooling favored the expansion of *Pediastrum* and *Nuphar ca.* 3,000 cal. yrs. BP, as observed in Alaska (Edwards et al., 2000). The Neoglacial was also characterized by landscape opening, as shown by a decrease in *Picea* and increase in Poaceae, also observed in previous studies (MacDonald, 1995; Pienitz et al., 1999). Lower fuel abundance, likely due to cooler and drier conditions less favorable to shrub and tree productivity, hindered fire spread leading to lower biomass burned.

Last millennium (1,000-0 cal. yrs. BP)

During the last 1,000 years, temperature varied but remained low until *ca.* 500 cal. yrs. BP before a marked increase, especially during the last century. Vegetation density and fire frequency were as low as during the early Holocene, while *RegBB* reached its lowest levels for the entire time series. Contrary to our expectations, the recent fire size/severity (i.e. over the last 500 years) is below the maximum values observed during the mid-Holocene.

4.2 Implications for future fire risk

We provide evidence that both climate conditions and vegetation dynamics played a key role in shaping the wildfire regime over the past 10,000 years in central NWT. Fire size and/or severity were higher under the warmer and wetter climate of the mid-Holocene (7,000 to 5,000 cal. yrs. BP), which favored fuel availability, corroborating recent observations on large wildfires during the last decades in

361 the study area (Gaboriau et al., under review). Our results can be used to anticipate future fire risk and to
362 elaborate risk mitigation strategies including fuel management.

363 While temperature is expected to continue increasing in western Canada over the 21st century,
364 dryness periods could be more severe than in the past (Price et al., 2013). Hence, fire frequency might
365 increase (Wotton et al., 2017), but not necessarily biomass burning. Indeed, temperature increase could
366 lead to the conversion of coniferous to deciduous forests (Hansen et al., in press; Mekonnen et al.,
367 2019), or to a more open landscape (Asselin and Payette, 2005; Baltzer et al., submitted), which would
368 negatively feedback on fire ignition and spread by reducing fuel flammability, combustibility, and/or
369 connectivity. Hence, for large wildfires to be frequent in the future, the warming-induced increase in
370 evapotranspiration will have to be compensated by increased precipitation to produce sufficient fuel
371 (Flannigan et al., 2016).

372 **5. Acknowledgements**

373 We thank Benoît Brossier, David Gervais, Julia Morarin, Laure Paradis and David Pretorius for their
374 assistance in the field. We are also grateful to Christine Simard for her help in identifying charcoal
375 fragments, Jordan Paillard for pollen counting and identification and Pierre J. H. Richard for suggestions
376 on an earlier draft. This work was supported by Polar Knowledge Canada (Grant # NST-1718-0014), the
377 Natural Sciences and Engineering Research Council of Canada, the Canadian Forest Service, the
378 National Geography Society (Grant # EC-386R-18), and the French University Institute (IUF).

379 Data and R codes used in this manuscript are available here.

380

381 **6. References**

Abatzoglou, J.T., Kolden, C.A., 2013. Relationships between climate and macroscale area burned in the western United States. International Journal of Wildland Fire 22, 1003–1020.
Adams, M.A., 2013. Mega-fires, tipping points and ecosystem services: managing forests and woodlands in an uncertain future. Forest Ecology and Management 294, 250–261.
Ali, A.A., Blarquez, O., Girardin, M.P., Hély, C., Tinquaut, F., El Guellab, A., Valsecchi, V., Terrier, A., Bremond, L., Genries, A., 2012. Control of the multimillennial wildfire size in boreal North America by spring climatic conditions. Proceedings of the National Academy of Sciences 109, 20966–20970.
Andrews, J.T., Mode, W.N., Webber, P.J., Miller, G.H., Jacobs, J.D., 1980. Report on the distribution of dwarf birches and present pollen rain, Baffin Island, NWT, Canada. Arctic 33, 50–58.
Asselin, H., Payette, S., 2005. Late Holocene opening of the forest tundra landscape in northern Québec, Canada. Global Ecology and Biogeography 14, 307–313.
Baltzer, J.L., Nicola, D., Walker, X.J., Greene, D.F., Mack, M.C., submitted. Fire and the decline of fire-adapted black spruce in the boreal forest. Science.
Berkes, F., Davidson-Hunt, I.J., 2006. Biodiversity, traditional management systems, and cultural landscapes: examples from the boreal forest of Canada. International Social Science Journal 58, 35–47.
Blaauw, M., 2010. Methods and code for 'classical'age-modelling of radiocarbon sequences. Quaternary Geochronology 5, 512–518.
Blaauw, M., Christen, J.A., 2011. Flexible paleoclimate age-depth models using an autoregressive gamma process. Bayesian analysis 6, 457–474.
Blarquez, O., Vannière, B., Marlon, J.R., Daniau, A.-L., Power, M.J., Brewer, S., Bartlein, P.J., 2014. paleofire: an R package to analyse sedimentary charcoal records from the Global Charcoal Database to reconstruct past biomass burning. Computers & Geosciences 72, 255–261.
Boer, M.M., de Dios, V.R., Bradstock, R.A., 2020. Unprecedented burn area of Australian mega forest fires. Nature Climate Change 10, 171–172.
Boulanger, Y., Taylor, A.R., Price, D.T., Cyr, D., McGarrigle, E., Rammer, W., Sainte-Marie, G., Beaudoin, A., Guindon, L., Mansuy, N., 2017. Climate change impacts on forest landscapes along the Canadian southern boreal forest transition zone. Landscape Ecology 32, 1415–1431.
Braadbaart, F., Poole, I., 2008. Morphological, chemical and physical changes during charcoalification of wood and its relevance to archaeological contexts. Journal of Archaeological Science 35, 2434–2445.
Brossier, B., Oris, F., Finsinger, W., Asselin, H., Bergeron, Y., Ali, A.A., 2014. Using tree-ring records to calibrate peak detection in fire reconstructions based on sedimentary charcoal records. Holocene 24, 635–645.
Campbell, I.D., McDonald, K., Flannigan, M.D., Kringayark, J., 1999. Long-distance transport of pollen into the Arctic. Nature 399, 29–30.
Cansler, C.A., McKenzie, D., 2014. Climate, fire size, and biophysical setting control fire severity and spatial pattern in the northern Cascade Range, USA. Ecological Applications 24, 1037–1056.
Carcaillet, C., Bouvier, M., Fréchette, B., Larouche, A.C., Richard, P.J., 2001. Comparison of pollen-slide and sieving methods in lacustrine charcoal analyses for local and regional fire history. Holocene 11, 467–476.
Chapin, F.S., McGuire, A.D., Ruess, R.W., Hollingsworth, T.N., Mack, M.C., Johnstone, J.F., Kasischke, E.S., Euskirchen, E.S., Jones, J.B., Jorgenson, M.T., 2010. Resilience of Alaska's boreal forest to climatic change. Canadian Journal of Forest Research 40, 1360–1370.

Chaste, E., Girardin, M.P., Kaplan, J.O., Bergeron, Y., Hély, C., 2019. Increases in heat-induced tree mortality could drive reductions of biomass resources in Canada's managed boreal forest. Landscape Ecology 34, 403–426.
Conedera, M., Tinner, W., Neff, C., Meurer, M., Dickens, A.F., Krebs, P., 2009. Reconstructing past fire regimes: methods, applications, and relevance to fire management and conservation. Quaternary Science Reviews 28, 555–576.
Coogan, S.C., Robinne, F.-N., Jain, P., Flannigan, M.D., 2019. Scientists' warning on wildfire—a Canadian perspective. Canadian Journal of Forest Research 49, 1015–1023.
Crann, C.A., Patterson, R.T., Macumber, A.L., Galloway, J.M., Roe, H.M., Blaauw, M., Swindles, G.T., Falck, H., 2015. Sediment accumulation rates in subarctic lakes: insights into age-depth modeling from 22 dated lake records from the Northwest Territories, Canada. Quaternary Geochronology 27, 131–144.
Cwynar, L., Spear, R., 1995. Paleovegetation and paleoclimatic changes in the Yukon at 6 ka BP. Géographie physique et Quaternaire 49, 29–35.
Dalton, A.S., Margold, M., Stokes, C.R., Tarasov, L., Dyke, A.S., Adams, R.S., Allard, S., Arends, H.E., Atkinson, N., Attig, J.W., 2020. An updated radiocarbon-based ice margin chronology for the last deglaciation of the North American Ice Sheet Complex. Quaternary Science Reviews 234, 106223.
De la Barrera, F., Barraza, F., Favier, P., Ruiz, V., Quense, J., 2018. Megafires in Chile 2017: Monitoring multiscale environmental impacts of burned ecosystems. Science of the Total Environment 637–638, 1526–1536. https://doi.org/10.1016/j.scitotenv.2018.05.119
Djamali, M., Cilleros, K., 2020. Statistically significant minimum pollen count in Quaternary pollen analysis; the case of pollen-rich lake sediments. Review of Palaeobotany and Palynology 275, 104156.
Dodd, W., Howard, C., Rose, C., Scott, C., Scott, P., Cunsolo, A., Orbinski, J., 2018. The summer of smoke: ecosocial and health impacts of a record wildfire season in the Northwest Territories, Canada. The Lancet Global Health 6, S30.
Duffy, P.A., Walsh, J.E., Graham, J.M., Mann, D.H., Rupp, T.S., 2005. Impacts of large-scale atmospheric–ocean variability on Alaskan fire season severity. Ecological Applications 15, 1317–1330.
Dyke, A., 2005. Late Quaternary vegetation history of northern North America based on pollen, macrofossil, and faunal remains. Géographie physique et Quaternaire 59, 211–262.
Edwards, M.E., Bigelow, N.H., Finney, B.P., Eisner, W.R., 2000. Records of aquatic pollen and sediment properties as indicators of late-Quaternary Alaskan lake levels. Journal of Paleolimnology 24, 55–68.
Environnement Canada, 2017. Canadian Climate Normals 1971-2000.
Erni, S., Arseneault, D., Parisien, M.-A., Bégin, Y., 2017. Spatial and temporal dimensions of fire activity in the fire-prone eastern Canadian taiga. Global Change Biology 23, 1152–1166.
Erni, S., Wang, X., Taylor, S., Boulanger, Y., Swystun, T., Flannigan, M., Parisien, M.-A., 2020. Developing a two-level fire regime zonation system for Canada. Canadian Journal of Forest Research 50, 259–273.
Faegri, K., Iversen, J., 1989. Textbook of Pollen Analysis, 4th ed. John Wiley & Sons Ltd., Chichester.
Flannigan, M., Cantin, A.S., De Groot, W.J., Wotton, M., Newbery, A., Gowman, L.M., 2013. Global wildland fire season severity in the 21st century. Forest Ecology and Management 294, 54–61.

Flannigan, M.D., Wotton, B.M., Marshall, G.A., De Groot, W.J., Johnston, J., Jurko, N., Cantin, A.S., 2016. Fuel moisture sensitivity to temperature and precipitation: climate change implications. Climatic Change 134, 59–71.

Fréchette, B., Richard, P.J., Grondin, P., Lavoie, M., Larouche, A.C., 2018. Histoire postglaciaire de la végétation et du climat des pessières et des sapinières de l'ouest du Québec, Mémoire de Recherche Forestière. Gouvernement du Québec, ministère des Forêts, de la Faune et des Parcs, Direction de la recherche forestière.

Gaboriau, D.M., Asselin, H., Ali, A.A., Hély, C., Girardin, M.P., under review. Main drivers of recent extreme wildfire years and identification of climatic thresholds on the territory of the Tłı̨chǫ First Nation, northwestern Canada. International Journal of Wildland Fire.

Gajewski, K., Bunbury, J., Vetter, M., Kroeker, N., Khan, A.H., 2014. Paleoenvironmental studies in southwestern Yukon. Arctic 67, 58–70.

Gajewski, K., Payette, S., Ritchie, J.C., 1993. Holocene vegetation history at the boreal-forest–shrub-tundra transition in north-western Quebec. Journal of Ecology 81, 433–443.

Glew, J.R., 1991. Miniature gravity corer for recovering short sediment cores. Journal of Paleolimnology 5, 285–287.

Hansen, W.D., Fitzsimmons, R., Olnes, J., Williams, A.P., in press. An alternate vegetation type proves resilient and persists for decades following forest conversion in the North American boreal biome. Journal of Ecology. https://doi.org/10.1111/1365-2745.13446

Hassol, S.J., 2005. Arctic Climate Impact Assessment - Scientific Report. Cambridge University Press.

Hély, C., Chaste, E., Girardin, M.P., Remy, C., Blarquez, O., Bergeron, Y., Ali, A.A., 2020. A Holocene perspective of vegetation controls on seasonal boreal wildfire sizes using numerical paleoecology. Frontiers in Forests and Global Change 3, 106.

Hennebelle, A., Aleman, J.C., Ali, A.A., Bergeron, Y., Carcaillet, C., Grondin, P., Landry, J., Blarquez, O., 2020. The reconstruction of burned area and fire severity using charcoal from boreal lake sediments. Holocene.

Higuera, P., 2009. CharAnalysis 0.9: diagnostic and analytical tools for sediment charcoal analysis. User's Guide, Montana State University, Bozeman, MT.

Hoecker, T.J., Higuera, P.E., Kelly, R., Hu, F.S., 2020. Arctic and boreal paleofire records reveal drivers of fire activity and departures from Holocene variability. Ecology 0, e03096.

IPCC, 2014. Climate Change 2014: Synthesis Report Summary for Policymakers. Contribution of Working Groups I, II and III to the Fifth Assessment Report of the Intergovernmental Panel on Climate Change.

Jain, P., Wang, X., Flannigan, M.D., 2018. Trend analysis of fire season length and extreme fire weather in North America between 1979 and 2015. International Journal of Wildland Fire 26, 1009–1020.

Juggins, S., 2017. Rioja: analysis of Quaternary science data. R package version (0.9–21).

Kasischke, E.S., Turetsky, M.R., 2006. Recent changes in the fire regime across the North American boreal region—Spatial and temporal patterns of burning across Canada and Alaska. Geophysical Research Letters 33, L09703.

Kaufman, D.S., Ager, T.A., Anderson, N.J., Anderson, P.M., Andrews, J.T., Bartlein, P.J., Brubaker, L.B., Coats, L.L., Cwynar, L.C., Duvall, M.L., 2004. Holocene thermal maximum in the western Arctic (0–180 W). Quaternary Science Reviews 23, 529–560.

Kelly, R., Chipman, M.L., Higuera, P.E., Stefanova, I., Brubaker, L.B., Hu, F.S., 2013. Recent burning of boreal forests exceeds fire regime limits of the past 10,000 years. Proceedings of the National Academy of Sciences 110, 13055–13060.

Kobashi, T., Menviel, L., Jeltsch-Thömmes, A., Vinther, B.M., Box, J.E., Muscheler, R., Nakaegawa, T., Pfister, P.L., Döring, M., Leuenberger, M., 2017. Volcanic influence on centennial to millennial Holocene Greenland temperature change. Scientific Reports 7.

Kochtubajda, B., Stewart, R.E., Flannigan, M.D., Bonsal, B.R., Cuell, C., Mooney, C.J., 2019. An assessment of surface and atmospheric conditions associated with the extreme 2014 wildfire season in Canada's Northwest Territories. Atmosphere-Ocean 57, 73–90.

Latifovic, R., Pouliot, D., Olthof, I., 2017. Circa 2010 land cover of Canada: Local optimization methodology and product development. Remote Sensing 9, 1098.

Lauriol, B., Lacelle, D., Labrecque, S., Duguay, C.R., Telka, A., 2009. Holocene evolution of lakes in the Bluefish Basin, northern Yukon, Canada. Arctic 62, 212–224.

Lecavalier, B.S., Fisher, D.A., Milne, G.A., Vinther, B.M., Tarasov, L., Huybrechts, P., Lacelle, D., Main, B., Zheng, J., Bourgeois, J., 2017. High Arctic Holocene temperature record from the Agassiz ice cap and Greenland ice sheet evolution. Proceedings of the National Academy of Sciences 114, 5952–5957.

MacDonald, G., 1995. Vegetation of the continental Northwest Territories at 6 ka BP. Géographie physique et Quaternaire 49, 37–43.

MacDonald, G.M., Edwards, T.W., Moser, K.A., Pienitz, R., Smol, J.P., 1993. Rapid response of treeline vegetation and lakes to past climate warming. Nature 361, 243–246.

Macumber, A.L., Neville, L.A., Galloway, J.M., Patterson, R.T., Falck, H., Swindles, G., Crann, C., Clark, I., Gammon, P., Madsen, E., 2011. Paleoclimatological Assessment of the Northwest Territories and Implications for the Long-Term Viability of the Tibbitt to Contwoyto Winter Road, Part II: March 2010 Field Season Results. Open report 2010-010. Northwest Territories. Geoscience office, NT.

Mann, M.E., Rahmstorf, S., Kornhuber, K., Steinman, B.A., Miller, S.K., Coumou, D., 2017. Influence of anthropogenic climate change on planetary wave resonance and extreme weather events. Scientific Reports 7.

Meehl, G.A., Stocker, T.F., Collins, W.D., Friedlingstein, P., Gaye, T., Gregory, J.M., Kitoh, A., Knutti, R., Murphy, J.M., Noda, A., 2007. Global climate projections.

Mekonnen, Z.A., Riley, W.J., Randerson, J.T., Grant, R.F., Rogers, B.M., 2019. Expansion of high-latitude deciduous forests driven by interactions between climate warming and fire. Nature Plants 5, 952–958.

Mooney, S.D., Tinner, W., 2011. The analysis of charcoal in peat and organic sediments. Mires and Peat 7, 1–18.

Moser, K.A., MacDonald, G.M., 1990. Holocene vegetation change at treeline north of Yellowknife, Northwest Territories, Canada. Quaternary Research 34, 227–239.

Motic Images, 2018. Motic Images Plus 3.0 ML Software.

Mudelsee, M., 2013. Climate time series analysis, classical statistical and bootstrap methods. Springer, Dordrecht.

Mustaphi, C.J.C., Davis, E.L., Perreault, J.T., Pisaric, M.F., 2015. Spatial variability of recent macroscopic charcoal deposition in a small montane lake and implications for reconstruction of watershed-scale fire regimes. Journal of Paleolimnology 54, 71–86.

Nolan, R.H., Boer, M.M., Collins, L., Resco de Dios, V., Clarke, H., Jenkins, M., Kenny, B., Bradstock, R.A., 2020. Causes and consequences of eastern Australia's 2019-20 season of mega-fires. Global Change Biology 26, 3756–3758. https://doi.org/10.1111/gcb.14987

NTENR, 2015. 2014 Fire season review report (No. 249– 17(5)). Legislative assembly of the Northwest Territories https://www.assembly.gov.nt.ca/sites/default/files/td_249-175.pdf.

563 Olson, D.M., Dinerstein, E., Wikramanayake, E.D., Burgess, N.D., Powell, G.V., Underwood, E.C.,
564 D'amico, J.A., Itoua, I., Strand, H.E., Morrison, J.C., 2001. Terrestrial ecoregions of the world: a
565 new map of life on Earth. BioScience 51, 933–938.
566 Oris, F., Ali, A.A., Asselin, H., Paradis, L., Bergeron, Y., Finsinger, W., 2014. Charcoal dispersion and
567 deposition in boreal lakes from 3 years of monitoring: differences between local and regional
568 fires. Geophysical Research Letters 41, 6743–6752.
569 Parisien, M.-A., Barber, Q.E., Hirsch, K.G., Stockdale, C.A., Erni, S., Wang, X., Arseneault, D., Parks,
570 S.A., 2020. Fire deficit increases wildfire risk for many communities in the Canadian boreal
571 forest. Nature Communications 11, 2121.
572 Pienitz, R., Smol, J.P., MacDonald, G.M., 1999. Paleolimnological reconstruction of Holocene climatic
573 trends from two boreal treeline lakes, Northwest Territories, Canada. Arctic, Antarctic, and
574 Alpine Research 31, 82–93.
575 Polanco-Martinez, J.M., Medina-Elizalde, M.A., Goni, M.F.S., Mudelsee, M., 2019. BINCOR: An R
576 package for Estimating the Correlation between Two Unevenly Spaced Time Series. R Journal
577 11, 170–184.
578 Porter, T.J., Schoenemann, S.W., Davies, L.J., Steig, E.J., Bandara, S., Froese, D.G., 2019. Recent
579 summer warming in northwestern Canada exceeds the Holocene thermal maximum. Nature
580 Communications 10, 1631.
581 Power, M.J., Marlon, J., Ortiz, N., Bartlein, P.J., Harrison, S.P., Mayle, F.E., Ballouche, A., Bradshaw,
582 R.H., Carcaillet, C., Cordova, C., 2008. Changes in fire regimes since the Last Glacial
583 Maximum: an assessment based on a global synthesis and analysis of charcoal data. Climate
584 Dynamics 30, 887–907.
585 Price, D.T., Alfaro, R.I., Brown, K.J., Flannigan, M.D., Fleming, R.A., Hogg, E.H., Girardin, M.P.,
586 Lakusta, T., Johnston, M., McKenney, D.W., 2013. Anticipating the consequences of climate
587 change for Canada's boreal forest ecosystems. Environmental Reviews 21, 322–365.
588 Reimer, P.J., Bard, E., Bayliss, A., Beck, J.W., Blackwell, P.G., Ramsey, C.B., Buck, C.E., Cheng, H.,
589 Edwards, R.L., Friedrich, M., 2013. IntCal13 and Marine13 radiocarbon age calibration curves
590 0–50,000 years cal. BP. Radiocarbon 55, 1869–1887.
591 Remy, C.C., Lavoie, M., Girardin, M.P., Hély, C., Bergeron, Y., Grondin, P., Oris, F., Asselin, H., Ali,
592 A.A., 2017. Wildfire size alters long-term vegetation trajectories in boreal forests of eastern
593 North America. Journal of Biogeography 44, 1268–1279.
594 Richard, P., 1970. Atlas pollinique des arbres et de quelques arbustes indigènes du Québec. Naturaliste
595 Canadien 97, l–34; 97-l6l; 24l–306.
596 Ritchie, J.C., 1985. Late-Quaternary Climatic and Vegetational Change in the Lower Mackenzie Basin,
597 Northwest Canada. Ecology 66, 612–621.
598 Ritchie, J.C., Cwynar, L.C., Spear, R.W., 1983. Evidence from north-west Canada for an early Holocene
599 Milankovitch thermal maximum. Nature 305, 126–128.
600 SFOR, 2018. News and views: the burning hot summer of 2018. Scandinavian Journal of Forest
601 Research 33, 724–727.
602 Smith, A., Schismenos, S., Stevens, G., Hutton, L., Chalaris, M., Emmanouloudis, D., 2019.
603 Understanding large-scale fire events: megafires in Attica, Greece and California, USA. United
604 Nations Major Group for Children and Youth, USA, pp. 29–34.
605 Stephens, S.L., Burrows, N., Buyantuyev, A., Gray, R.W., Keane, R.E., Kubian, R., Liu, S., Seijo, F.,
606 Shu, L., Tolhurst, K.G., 2014. Temperate and boreal forest mega-fires: characteristics and
607 challenges. Frontiers in Ecology and the Environment 12, 115–122.
608 https://doi.org/10.1890/120332

609 Sulphur, K.C., Goldsmith, S.A., Galloway, J.M., Macumber, A., Griffith, F., Swindles, G.T., Patterson,
610 R.T., Falck, H., Clark, I.D., 2016. Holocene fire regimes and treeline migration rates in sub-
611 arctic Canada. Global and Planetary Change 145, 42–56.
612 Swain, A.M., 1973. A history of fire and vegetation in Northeastern Minnesota as recorded in lake
613 sediments. Quaternary Research 3, 383–390.
614 Timoney, K.P., Mamet, S.D., Cheng, R., Lee, P., Robinson, A.L., Downing, D., Wein, R.W., 2019. Tree
615 cover response to climate change in the forest-tundra of north-central Canada: fire-driven
616 decline, not northward advance. Ecoscience 26, 133–148.
617 Tinner, W., Hu, F.S., Beer, R., Kaltenrieder, P., Scheurer, B., Krähenbühl, U., 2006. Postglacial
618 vegetational and fire history: pollen, plant macrofossil and charcoal records from two Alaskan
619 lakes. Vegetation History and Archaeobotany 15, 279–293.
620 Trachsel, M., Telford, R.J., 2017. All age–depth models are wrong, but are getting better. Holocene 27,
621 860–869.
622 Turco, M., von Hardenberg, J., AghaKouchak, A., Llasat, M.C., Provenzale, A., Trigo, R.M., 2017. On
623 the key role of droughts in the dynamics of summer fires in Mediterranean Europe. Scientific
624 Reports 7, 81.
625 Upiter, L.M., Vermaire, J.C., Patterson, R.T., Crann, C.A., Galloway, J.M., Macumber, A.L., Neville,
626 L.A., Swindles, G.T., Falck, H., Roe, H.M., 2014. Middle to late Holocene chironomid-inferred
627 July temperatures for the central Northwest Territories, Canada. Journal of Paleolimnology 52,
628 11–26.
629 Veraverbeke, S., Rogers, B.M., Goulden, M.L., Jandt, R.R., Miller, C.E., Wiggins, E.B., Randerson,
630 J.T., 2017. Lightning as a major driver of recent large fire years in North American boreal
631 forests. Nature Climate Change 7, 529–534.
632 Viau, A.E., Gajewski, K., 2009. Reconstructing millennial-scale, regional paleoclimates of boreal
633 Canada during the Holocene. Journal of Climate 22, 316–330.
634 Viau, A.E., Gajewski, K., Sawada, M.C., Fines, P., 2006. Millennial-scale temperature variations in
635 North America during the Holocene. Journal of Geophysical Research: Atmospheres 111,
636 D09102.
637 Vincent, J.-S., 1973. A palynological study for the Little Clay Belt, northwestern Quebec. Naturaliste
638 Canadien 100, 59–70.
639 Walker, X.J., Baltzer, J.L., Cumming, S.G., Day, N.J., Johnstone, J.F., Rogers, B.M., Solvik, K.,
640 Turetsky, M.R., Mack, M.C., 2018. Soil organic layer combustion in boreal black spruce and
641 jack pine stands of the Northwest Territories, Canada. International Journal of Wildland Fire 27,
642 125–134.
643 Wang, X., Parisien, M.-A., Taylor, S.W., Candau, J.-N., Stralberg, D., Marshall, G.A., Little, J.M.,
644 Flannigan, M.D., 2017. Projected changes in daily fire spread across Canada over the next
645 century. Environmental Research Letters 12, 025005.
646 Wang, Y., Hogg, E.H., Price, D.T., Edwards, J., Williamson, T., 2014. Past and projected future changes
647 in moisture conditions in the Canadian boreal forest. Forestry Chronicle 90, 678–691.
648 Williams, J.W., 2006. An atlas of pollen-vegetation-climate relationships for the United States and
649 Canada. American Association of Stratigraphic Palynologists Foundation, Dallas, Texas.
650 Winkler, M.G., 1985. Charcoal analysis for paleoenvironmental interpretation: a chemical assay.
651 Quaternary Research 23, 313–326.
652 Wotton, B.M., Flannigan, M.D., Marshall, G.A., 2017. Potential climate change impacts on fire intensity
653 and key wildfire suppression thresholds in Canada. Environmental Research Letters 12, 095003.

654 Zhang, X., Brown, R., Vincent, L., Skinner, W., Feng, Y., Mekis, E., 2011. Canadian climate trends,
655 1950–2007, in: Canadian Biodiversity: Ecosystem Status and Trends 2010, Technical Thematic
656 Report No. 5. Canadian Councils of Resource Ministers, Ottawa, ON.

Table 1. Characteristics of the four studied lakes and sediment records.

Lakes	**Emile**	**Izaac**	**Paradis**	**Saxon**

Characteristics				
Latitude (°N)	64°03’16.64”	64°05’56.21”	64°00’23.54”	63°48’26.06”
Longitude (°W)	114°06’21.67”	114°10’33.08”	114°59’19.24”	114°58’33.29”
Surface area (ha)	1.4	1.5	1.8	0.9
Elevation (m above sea level)	393	394	347	392
Maximum water depth (cm)	150	115	235	540
Maximum length (m)	203	162	271	177
Lakeshores (**F**lat / **A**brupt)	F	F	F	A
Fluvial input (**P**resent / **A**bsent)	A	A	A	A
Date of the last local fire (CNFD)	2014	2014	1979	1998
Sediment records				
Total length of sediment (cm)	456	359	450	395
Depth of the basal ^{14}C date (cm)	448	340	441	350
Sedimentation rate (cm year^{-1})	0.049	0.036	0.046	0.036
Median signal-to-noise index	5.4	4.2	4.1	3.7
Total number of significant fire events	57	49	55	46

Table 2. BINCOR Pearson correlation coefficient (with 95% confidence interval) between fire metrics, temperature, total pollen accumulation rate (PAR), and accumulation rates of taxa with an average percentage greater than 0.1% over the entire study period. *** p < 0.001, ** p < 0.01 and * p < 0.05.

	RegFF	***RegBB***	***FS* index**	**Temperature**
Temperature	-0.53 [-0.63, -0.42]***	0.21 [0.07, 0.35]**	0.66 [0.58, 0.74]***	-
PAR	0.50 [0.35, 0.62]***	0.58 [0.45, 0.68]***	0.14 [-0.04, 0.31]	-0.13 [-0.30, 0.04]
Picea	0.37 [0.21, 0.51]***	0.64 [0.53, 0.74]***	0.29 [0.12, 0.44]***	0.00 [-0.17, 0.17]
Pinus	0.63 [0.52, 0.72]***	-0.16 [-0.32, 0.00]	-0.56 [-0.67, -0.44]***	-0.52 [-0.63, -0.39]***
Betula	0.27 [0.12, 0.42]***	0.31 [0.16, 0.45]***	0.09 [-0.08, 0.25]	-0.06 [-0.22, 0.1]
Populus	-0.34 [-0.47, -0.18]***	0.04 [-0.13, 0.20]	0.28 [0.12, 0.43]***	0.18 [0.02, 0.34]*
Alnus alnobetula* subsp. *crispa	0.40 [0.25, 0.53]***	0.42 [0.28, 0.55]***	0.09 [-0.08, 0.25]	-0.02 [-0.18, 0.14]
Alnus incana* subsp. *rugosa	0.23 [0.07, 0.38]**	0.16 [0.00, 0.32]*	-0.02 [-0.18, 0.15]	-0.14 [-0.30, 0.02]
Juniperus	0.09 [-0.08, 0.25]	-0.30 [-0.45, -0.15]***	-0.33 [-0.47, -0.17]***	-0.38 [-0.51, -0.23]***
Salix	0.21 [0.05, 0.36]*	0.10 [-0.06, 0.26]	-0.04 [-0.21, 0.12]	-0.17 [-0.32, -0.01]*
Larix	0.21 [0.05, 0.36]*	-0.23 [-0.38, -0.07]**	-0.34 [-0.48, -0.19]***	-0.26 [-0.41, -0.1]**
Cyperaceae	0.20 [0.03, 0.35]*	-0.01 [-0.17, 0.15]	-0.13 [-0.29, 0.03]	-0.19 [-0.34, -0.03]*
Ericaceae	0.14 [-0.03, 0.29]	0.11 [-0.06, 0.27]	0.00 [-0.16, 0.17]	0.01 [-0.15, 0.17]
Artemisia	-0.05 [-0.22, 0.11]	0.10 [-0.06, 0.26]	0.13 [-0.04, 0.29]	0.15 [-0.01, 0.31]
Myrica	-0.46 [-0.58, -0.32]***	-0.01 [-0.17, 0.16]	0.33 [0.17, 0.47]***	0.38 [0.23, 0.51]***
Lycopodium	-0.31 [-0.45, -0.15]***	-0.05 [-0.21, 0.12]	0.19 [0.03, 0.35]*	0.2 [0.04, 0.35]*
Poaceae	0.23 [0.07, 0.38]**	-0.04 [-0.21, 0.12]	-0.19 [-0.34, -0.02]*	-0.24 [-0.39, -0.08]**
Pediastrum	0.28 [0.12, 0.43]***	-0.23 [-0.38, -0.07]**	-0.37 [-0.5, -0.22]***	-0.23 [-0.38, -0.07]**
Potamogeton	-0.14 [-0.30, 0.02]	0.14 [-0.02, 0.30]	0.22 [0.06, 0.37]**	0.10 [-0.06, 0.26]
Nuphar	0.38 [0.23, 0.51]***	0.01 [-0.15, 0.18]	-0.24 [-0.39, -0.08]**	-0.24 [-0.39, -0.08]**

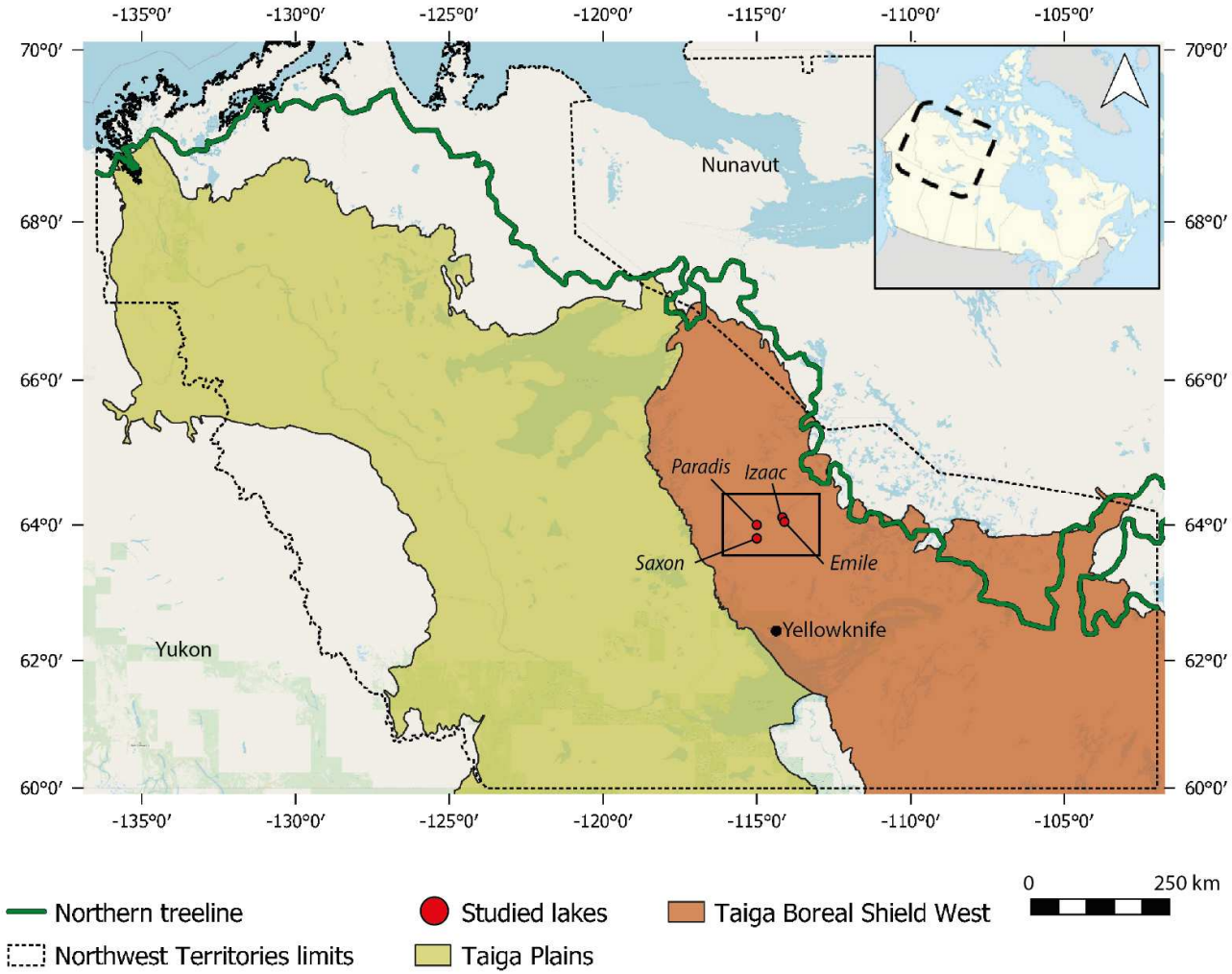

Figure 1. Locations of the studied lakes in the Northwest Territories (north-central Canada), showing ecozones (adapted from Olson et al., 2001) and treeline (adapted from Timoney et al., 2019).

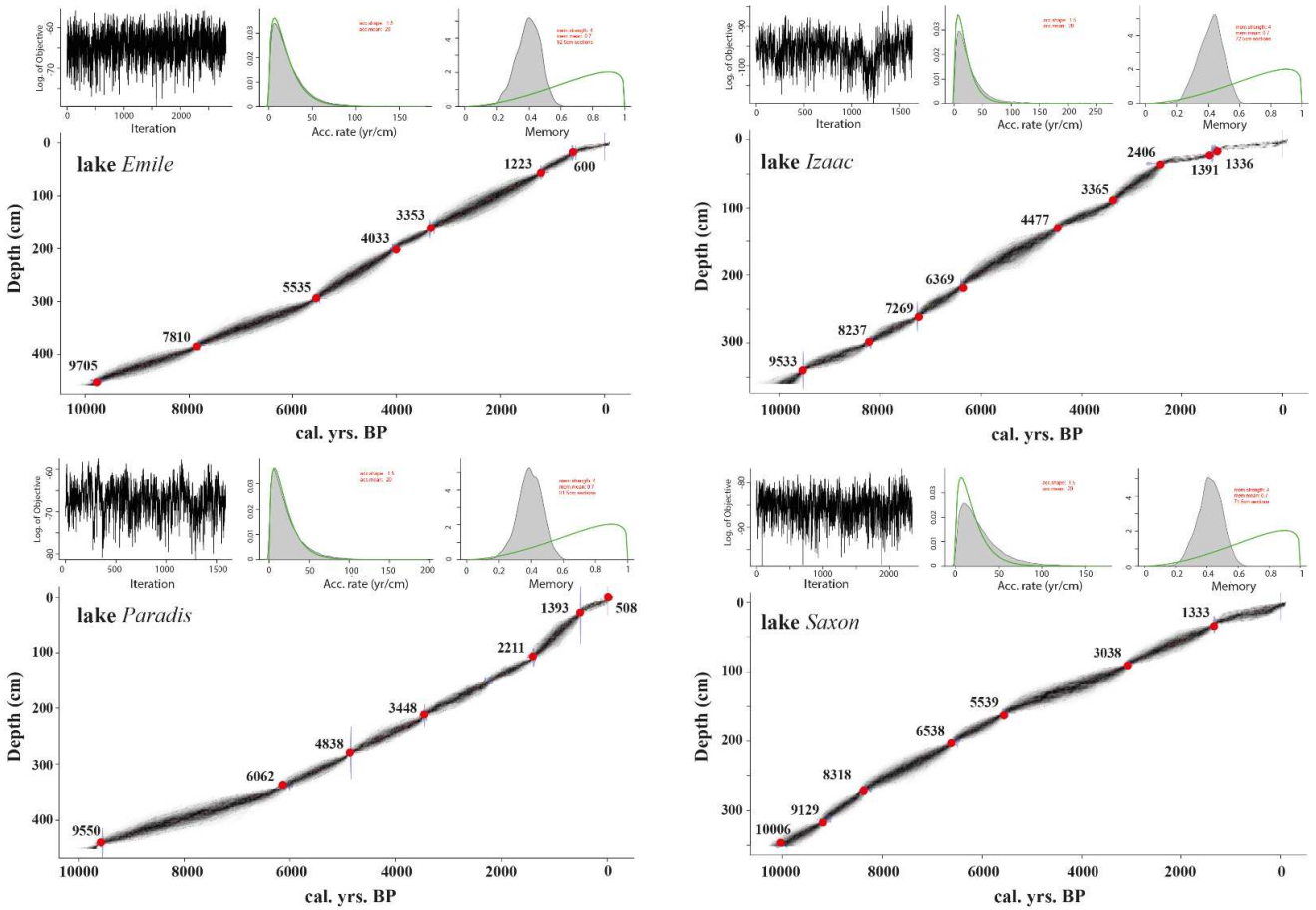

Figure 2. WinBacon outputs for lakes *Emile*, *Izaac*, *Paradis* and *Saxon*. Upper left panels describe the MCMC (Markov Chain Monte Carlo) iterations (the distribution is stationary with little structure among neighbouring iterations). Upper middle panels show the distribution of sediment accumulation rates. Upper right panels show the memory corresponding to the variation of sediment accumulation rate in time. Main panels show the calibrated ^{14}C dates (see Table S1 for full details on the chronology) and age-depth models (with 95% confidence intervals).

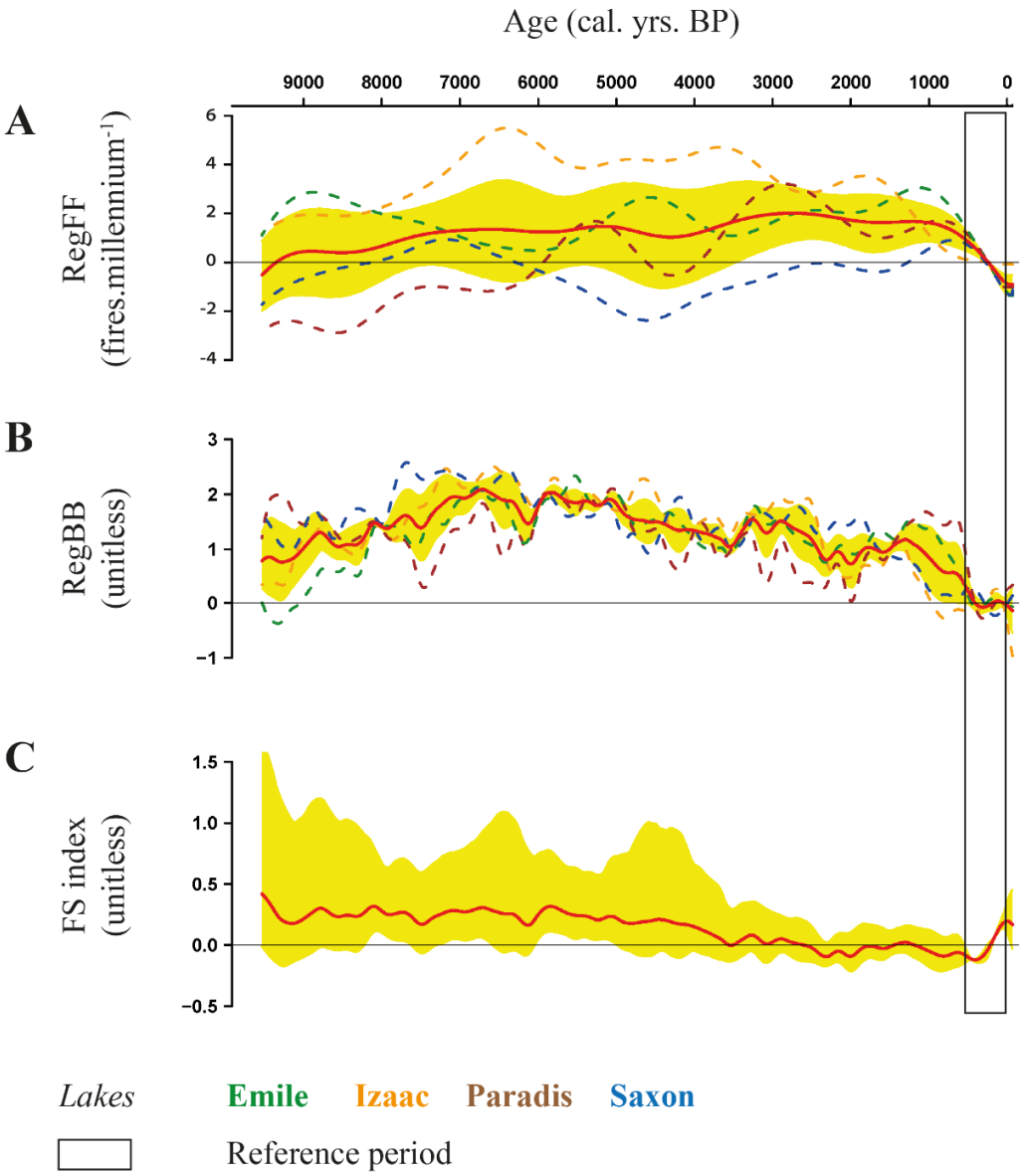

Figure 3. Holocene fire activity anomalies interpolated using a 500-year bandwidth smoothing, relative to the 500-0 cal. yrs. BP reference period (black horizontal line) for individual and regional fire-history reconstructions based on sediment charcoal records from lakes *Emile*, *Izaac*, *Paradis* and *Saxon*: (A) Regional Fire Frequency (*RegFF*), (B) Regional Biomass Burning (*RegBB*) and (C) Fire Size/Severity (*FS* index) based on regional biomass burning and fire frequency. Yellow shaded areas in each panel represent the 90% bootstrap confidence intervals.

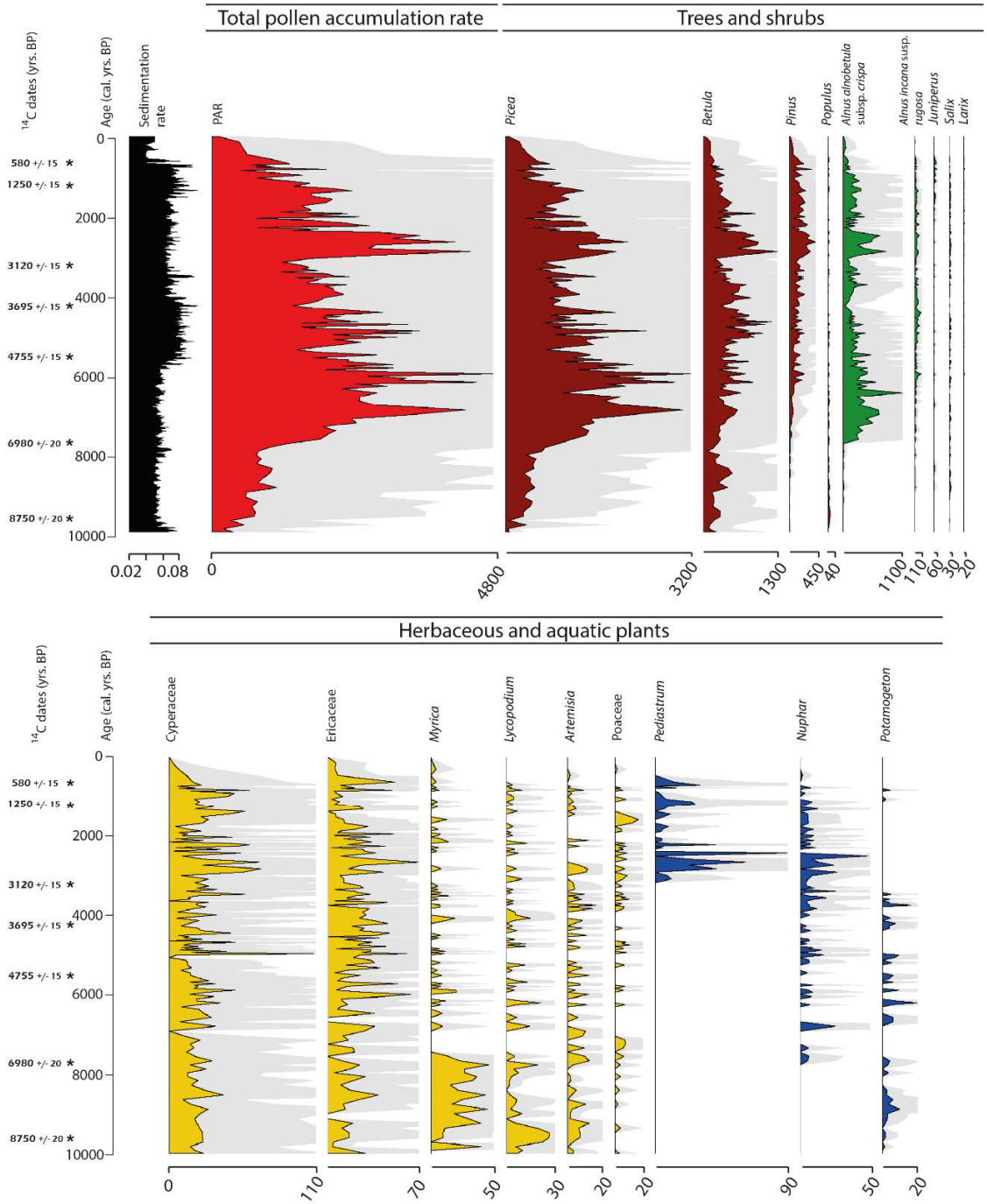

Figure 4. Sedimentation (cm^{-1} $year^{-1}$) and pollen accumulation rates (grains cm^{-2} $year^{-1}$) at lake *Emile* for total terrestrial pollen (PAR, in red) and for the main taxa: trees (in brown), shrubs (in green), herbaceous plants (in yellow) and green algae (*Coenobium*) and aquatic plants (in blue) all having an average percentage greater than 0.1% over the entire study period. Pale areas represent × 5 exaggeration. Note that the scale differs for each pollen or spore taxon.

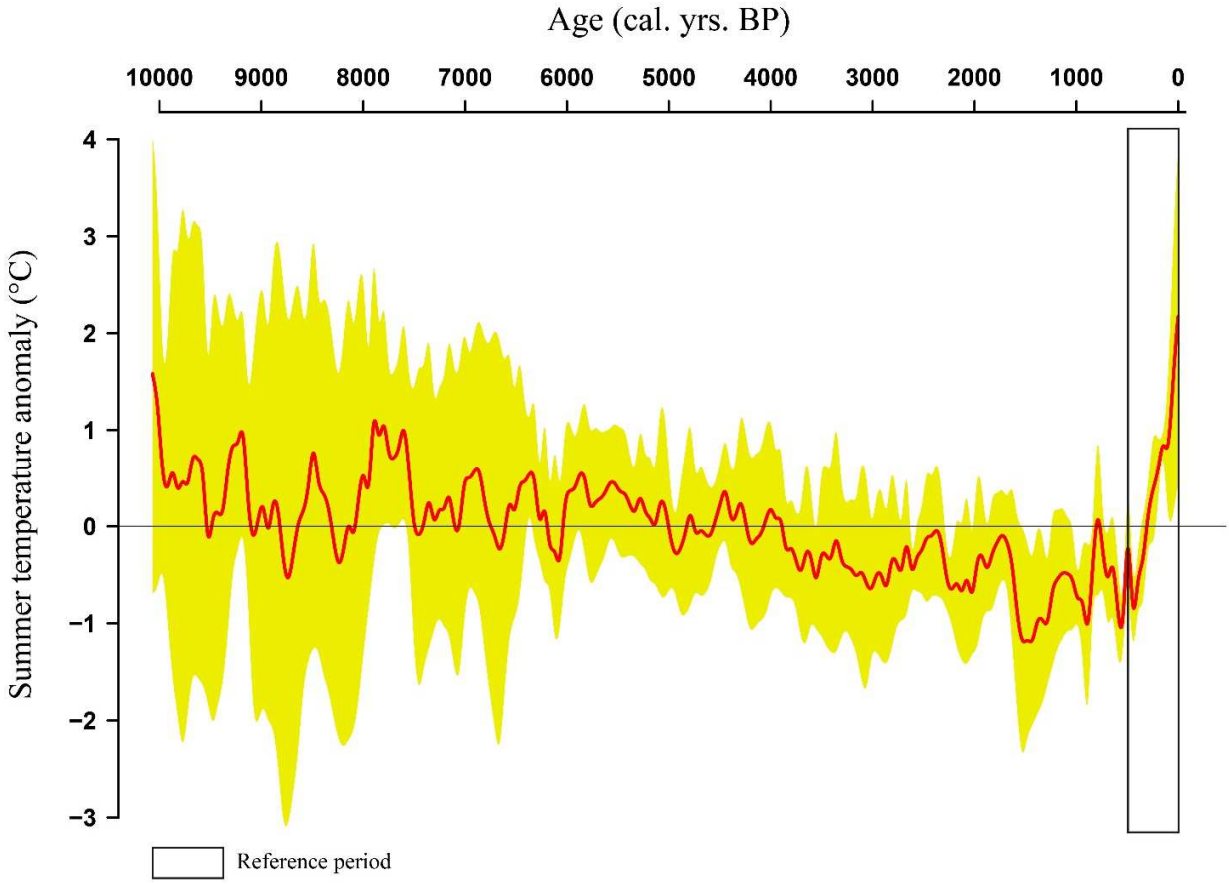

Figure 5. Mean summer temperature anomalies over the Holocene, relative to the 500-0 cal. yrs. BP reference period, obtained from the calculation of the means of standardized independent temperature datasets described in Appendix S4. The yellow shaded area indicates the 90% bootstrap confidence interval.

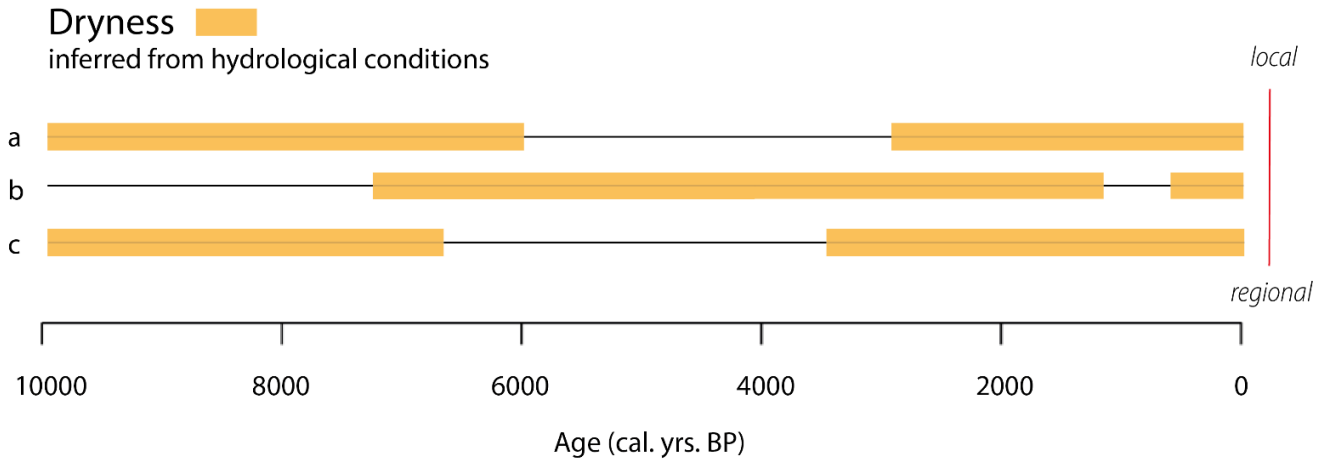

Figure 6. Dryness periods inferred from hydrological conditions from different locations in north-central and northwestern Canada. Distance from the study area increases from top to bottom. (*a*) Central Northwest Territories (Pienitz et al., 1999; dissolved organic carbon (DOC) inferred form diatom assemblages). (*b*) Mackenzie region (50°-70°N, 120°-140°W; Viau and Gajewski, 2009; annual precipitation inferred from pollen assemblages). (*c*) Northern Yukon (Lauriol et al., 2009; lake-level inferred from plant macrofossil analysis).